Design of an Activity-Based Probe for Human Neutrophil Elastase: Implementation of the Lossen Rearrangement to Induce Förster Resonance Energy Transfers

Journal:	*Biochemistry*
Manuscript ID	bi-2017-009066.R2
Manuscript Type:	Article
Date Submitted by the Author:	n/a
Complete List of Authors:	Schulz-Fincke, Anna-Christina; University of Bonn, Pharmaceutical Institute Tikhomirov, Alexander; Gause Instituteof new Antibiotics Braune, Annett; German Institute of Human Nutrition Potsdam-Rehbruecke, Gastrointestinal Microbiology Girbl, Tamara; Queen Mary University of London, William Harvey Research Institute Gilberg, Erik; LIMES Program Unit Chemical Biology and Medicinal Chemistry, Department of Life Science Informatics Bajorath, Jürgen; University of Bonn, Life Science Informatics, B-IT; University of Bonn, Department of Life Science Informatics Blaut, Michael; German Institute of Human Nutrition, Dept. of Gastrointestinal Microbiology Nourshargh, Sussan; Queen Mary University of London, William Harvey Research Institute Gütschow, Michael; University of Bonn, Pharmaceutical Institute

Design of an Activity-Based Probe for Human Neutrophil Elastase: Implementation of the Lossen Rearrangement to Induce Förster Resonance Energy Transfers

Anna-Christina Schulz-Fincke,[§] Alexander S. Tikhomirov,[§,†] Annett Braune,[‡] Tamara Girbl,[∞] Erik Gilberg,[§,#] Jürgen Bajorath,[#] Michael Blaut,[‡] Sussan Nourshargh,[∞] and Michael Gütschow[§,]*

[§] Pharmaceutical Institute, Pharmaceutical Chemistry I, University of Bonn, An der Immenburg 4, 53121 Bonn, Germany

[†] Gause Institute of New Antibiotics, 11 Bolshaya Pirogovskaya Street, Moscow 119021, Russia

[‡] Department of Gastrointestinal Microbiology, German Institute of Human Nutrition Potsdam-Rehbruecke, Arthur-Scheunert-Allee 114–116, 14558 Nuthetal, Germany

[∞] William Harvey Research Institute, Barts and The London School of Medicine and Dentistry, Queen Mary University of London, Charterhouse Square, London EC1M 6BQ, UK

[#] Department of Life Science Informatics, B-IT, LIMES Program Unit Chemical Biology and Medicinal Chemistry, University of Bonn, Dahlmannstr. 2, 53113 Bonn, Germany.

KEYWORDS

Activity-based probes, elastase, enzyme inhibition, FRET, Lossen rearrangement

ABSTRACT

Human neutrophil elastase is an important regulator of the immune response and plays a role in host defense mechanisms and further physiological processes. The uncontrolled activity of this serine protease may cause severe tissue alterations and impair inflammatory states. The design of an activity-based probe for human neutrophil elastase reported herein relies on a sulfonyloxyphthalimide moiety as a new type of warhead which was linker-connected to a coumarin fluorophore. The inhibitory potency of the activity-based probe was assessed against several serine and cysteine proteases and selectivity for human neutrophil elastase (K_i = 6.85 nM) was determined. The adequate fluorescent tag of the probe allowed for the in-gel fluorescence detection of human neutrophil elastase in the low nanomolar range. The coumarin moiety and the anthranilic acid function of the probe, produced in the course of a Lossen rearrangement, were part of two different Förster resonance energy transfers.

TABLE OF CONTENT

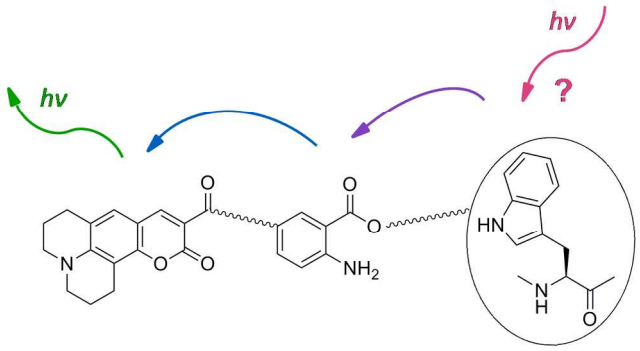

INTRODUCTION

Human neutrophil elastase (HNE) belongs to the chymotrypsin family of serine proteases and is primarily localized in the azurophilic granules and released upon stimulation of the polymorphonuclear neutrophils. HNE has a shallow S1 pocket resulting in a primary substrate specificity for small aliphatic residues, *e.g.* of alanine, isoleucine or valine, in the P1 position of the substrate. As a serine protease, HNE cleaves its substrates following an acyl transfer mechanism.[1] HNE exhibits a broad substrate specificity. It cleaves fibrous elastin, a highly elastic protein in connective tissues, as well as fibronectin, laminin and collagens. Besides these extracellular matrix proteins, HNE degrades a variety of plasma proteins, activates other proteases or deactivates their endogenous inhibitors and liberates growth factors.[1]

HNE participates in host defense against microbial pathogens due to its capability of cleaving outer membrane proteins of Gram-negative bacteria. A fusion of azurophilic granules with vacuoles carrying phagocytosed bacteria leads to the formation of phagolysosomes, the site of pathogen clearance.[1] In addition to intracellular defense mechanisms, HNE exerts an extracellular antimicrobial activity. It serves as a component of the neutrophil extracellular traps, a network of chromatin and granule proteins, which is actively secreted by neutrophils.[1,2]

In pathophysiological conditions, a deleterious effect may result from the extended tissue destruction catalyzed by HNE. Upon neutrophil activation at inflammatory sites, HNE is abundantly released into the intercellular space, thereby activating proinflammatory mediators and recruiting further neutrophils. Thus, the out-of-balance activity of HNE contributes to the onset and progression of several inflammatory disorders, among them chronic obstructive pulmonary disease, respiratory distress syndrome (ARDS), acute lung injury (ALI), cystic fibrosis and rheumatoid arthritis.[1]

Upon neutrophil activation by cytokines, chemoattractants or bacterial lipopolysaccharides, HNE is secreted into the extracellular space, and a fraction of the proteolytically active enzyme remains associated with the outer surface of the plasma membrane of neutrophils. In particular, the lipid leukotriene B_4 (LTB_4) is known to efficiently induce both cell surface presentation of HNE and HNE release into the environment. The activation of the LTB_4-HNE axis can promote the cleavage of adhesion molecules and drive remote organ damage.[3]

Potent and selective HNE inhibitors could prove therapeutically useful to reduce or treat HNE-dependent disorders. Sivelestat has reached the market for the treatment of ALI/ARDS in Japan and South Korea. Sivelestat has been reported to interact with HNE in a substrate-like manner. The drug's ester bond undergoes an enzymatic cleavage, a pivaloyl residue is transferred to the active site serine and the resulting acyl enzyme is proposed to undergo hydrolysis.[4] Other inhibitors of HNE comprise, *e.g.* peptidic trifluoromethyl ketones and phosphonates,[5] 4*H*-3,1-benzoxazin-ones,[6] azetidine-2,4-diones and saccharines,[7] kojic acid derivatives,[8] cyanobacterial cyclic peptides and depsipeptides.[9] Several classes of structurally-diverse heterocyclic HNE inhibitors, including 2-pyridones (*e.g.* AZD9668) and 3,4-dihydropyrimidin-2(1*H*)-ones (*e.g.* BAY-678), have been reported.[1]

Due to the protease's involvement in several diseases and its role as a pathogenic mediator in pulmonary disorders, HNE inhibition has become an important pharmaceutical option. Aside its role as a drug target, HNE-generated fragments of elastin and, recently, HNE itself have been described to be biomarkers for certain elastase-related conditions.[10] Moreover, activity-based probes (ABPs) for HNE are considered to be valuable for the detection and detailed investigation of this protease. In general, ABPs for serine proteases have emerged as powerful tools in life science.[11] ABPs enlarge the repertoire of methods, of which Western blotting is particularly

important, for detecting a certain protein. ABPs are active site-directed compounds and can selectively visualize the enzyme of interest in complex biological samples. Different electrophilic structures have been employed as warheads for the assembly of ABPs for HNE, *i.e.* isocoumarins,[12] sulfonyl fluorides,[13] azetidine-2,4-diones,[14] and phosphonates.[15]

Förster resonance energy transfer (FRET) constitutes a powerful tool for the visualization of protein activities.[16] In the present study, we conducted the design, synthesis, photophysical and biological evaluation of a fluorescent ABP for HNE equipped with a sulfonyloxyphthalimide moiety. We demonstrate that this warhead is capable to trigger appropriate FRET signals to study the enzyme-probe interaction.

MATERIALS AND METHODS

General. Melting points were determined on a Büchi 50 oil bath apparatus. Thin layer chromatography was performed using Merck aluminium sheets coated with silica gel 60 F_{254}. NMR spectra were recorded using Bruker Avance III-600 MHz and Bruker Avance DRX-500 MHz instruments. LC-DAD chromatograms and ESI-MS spectra were recorded on an Agilent 1100 HPLC system with an Applied Biosystems API-2000 mass spectrometer. HRMS was performed on a microTOF-Q mass spectrometer (Bruker, Köln, Germany) with ESI-source coupled with a HPLC Dionex Ultimate 3000 (Thermo Scientific, Braunschweig, Germany) using a EC50/2 Nucleodur C18 Gracity 3 µm column (Macherey-Nagel, Düren, Germany). A volume of one µL of a sample solution (1.0 mg/mL) was injected. Mobile phase was a mixture of 2 mM aqueous ammonium acetate solution and acetonitrile. Elution was performed from 90:10 up to 0:100 in 9 min, 0:100 for 5 min. Elemental analysis was performed with a vario MICRO

apparatus. Absorption spectra were recorded on Varian Cary 50 Bio, emission spectra on a Monaco Safas spectrofluorometer flx.

General Enzymatic Methods. Enzyme activities were assayed spectrophotometrically on a Varian Cary 50 Bio or on a Varian Cary 100 Bio device, respectively. Fluorometric assays were monitored on a FLUOstar Optima plate reader from BMG Labtech (Offenburg, Germany) in 96 well plates. FRET kinetics was monitored on a Monaco Safas spectrofluorometer flx. HNE, PPE, human thrombin and human cathepsin B were obtained from Calbiochem (Darmstadt, Germany), bovine chymotrypsin, bovine factor Xa and bovine trypsin from Sigma Aldrich, Germany, and human cathepsin L from Enzo Life Science (Lörrach, Germany). MeOSuc-Ala-Ala-Pro-Val-pNA was purchased from Calbiochem (Darmstadt, Germany), Suc-Ala-Ala-Pro-Phe-pNA, Z-Gly-Gly-Arg-AMC, Boc-Ile-Glu-Gly-Arg-AMC, Suc-Ala-Ala-Pro-Arg-pNA, Z-Arg-Arg-pNA, Z-Phe-Arg-pNA were from Bachem (Bubendorf, Switzerland). Reactions were monitored for 60 min unless stated otherwise. Experiments were performed in duplicate with five different inhibitor concentrations.

Enzyme Inhibition Assays. *Human Neutrophil Elastase.*[17] Assay buffer was 50 mM sodium phosphate buffer containing 500 mM NaCl, pH 7.8. An enzyme stock solution of 50 µg/mL was prepared in 100 mM sodium acetate buffer, pH 5.5. An aliquot was kept at 0°C and diluted with assay buffer directly before the measurement. A 50 mM stock solution of the chromogenic substrate MeOSuc-Ala-Ala-Pro-Val-pNA in DMSO was diluted with assay buffer containing 10% DMSO. The final concentrations were as follows: substrate, 100 µM (= 1.85 × K_m); DMSO, 1.5%; HNE, 35 ng/mL. Into a cuvette containing 890 µL assay buffer, 10 µL inhibitor solution in DMSO and 50 µL substrate solution were added and thoroughly mixed. The reaction was performed at 25 °C, initiated by adding 50 µL of the enzyme solution and monitored at 405 nm.

Porcine Pancreatic Elastase. Assay buffer was 50 mM sodium phosphate buffer containing 500 mM NaCl, pH 7.8. An enzyme stock solution of 100 U/mL was prepared in 100 mM sodium acetate buffer, pH 5.5. An aliquot was kept at 0°C and diluted with assay buffer directly before the measurement. A 50 mM stock solution of the chromogenic substrate MeOSuc-Ala-Ala-Pro-Val-pNA was prepared in DMSO and diluted with assay buffer containing 10% DMSO. In accordance to literature,[18] a K_m value greater than 1000 µM was determined with 18 different substrate concentrations in triplicate measurements. For the inhibition assay, the final concentrations were as follows: substrate, 100 µM ($<< K_m$); DMSO, 1.5%; PPE, 0.01 U/mL. Into a cuvette containing 890 µL assay buffer, 10 µL inhibitor solution in DMSO and 50 µL substrate solution were added and thoroughly mixed. The reaction was performed at 25 °C, initiated by adding 50 µL of the enzyme solution and monitored at 405 nm.

Bovine Chymotrypsin.[19] Assay buffer was 20 mM Tris-HCl buffer containing 150 mM NaCl, pH 8.4. An enzyme stock solution of 1 mg/mL was prepared in 1 mM aqueous HCl, diluted with assay buffer and kept at 0°C. A 40 mM stock solution of chromogenic substrate Suc-Ala-Ala-Pro-Phe-pNA was prepared in DMSO and diluted with assay buffer containing 10% DMSO. The final concentrations were as follows: substrate, 200 µM ($= 2.68 \times K_m$);[20] DMSO, 6%; chymotrypsin, 50 ng/mL. Into a cuvette containing 845 µL assay buffer, 55 µL inhibitor solution in DMSO and 50 µL 4 mM substrate solution were added and thoroughly mixed. The reaction was performed at 25 °C, initiated by adding 50 µL of the enzyme solution and monitored at 405 nm.

Human Thrombin.[21] Assay buffer was 50 mM Tris–HCl containing 150 mM NaCl, pH 8.0. The enzyme stock solution (10000 U/mL) was prepared in water, diluted with assay buffer and kept at 0°C. A 10 mM stock solution of the fluorogenic substrate Z-Gly-Gly-Arg-AMC in

DMSO was diluted with assay buffer. The final concentrations were as follows: substrate, 40 μM (= 1.00 × K_m); DMSO, 6%; thrombin, 1.5 U/mL. Into each well containing 173.8 μL assay buffer, 11.2 μL inhibitor solution in DMSO and 10 μL substrate solution were added and thoroughly mixed. The reaction was performed at 25 °C, initiated by adding 5 μL of the enzyme solution and monitored with an excitation wavelength of 340 nm and emission wavelength of 460 nm.

Bovine Factor Xa.[22] Assay buffer was 50 mM Tris-HCl containing 100 mM NaCl and 10 mM $CaCl_2$, pH 8.0. The enzyme stock solution (1 U/μL) was prepared in water, diluted with assay buffer (1:50) and kept at 0°C. A 20 mM stock solution of fluorogenic substrate Boc-Ile-Glu-Gly-Arg-AMC · AcOH in DMSO was diluted with assay buffer. The final concentrations were as follows: substrate, 100 μM (= 1.69 × K_m); DMSO, 6%; factor Xa, 0.5 U/mL. Into each well containing 174 μL assay buffer, 11 μL inhibitor solution in DMSO and 10 μL substrate solution were added and thoroughly mixed. The reaction was performed at 25 °C, initiated by adding 5 μL of the enzyme solution and monitored over 45 min with an excitation wavelength of 340 nm and emission wavelength of 460 nm.

Bovine Trypsin.[23] Assay buffer was 20 mM Tris-HCl containing 150 mM NaCl, pH 8.4. The trypsin stock solution (10 μg/mL) was prepared in 1 mM HCl, diluted with assay buffer and kept at 0°C. A 40 mM stock solution of the chromogenic substrate Suc-Ala-Ala-Pro-Arg-pNA in DMSO was diluted with assay buffer. The final concentrations were as follows: substrate, 200 μM (= 2.70 × K_m); DMSO, 6%; bovine trypsin, 40 ng/mL. Into a cuvette containing 845 μL assay buffer, 50 μL 4 mM substrate solution and 55 μL inhibitor solution in DMSO were added and thoroughly mixed. The reaction was performed at 25 °C, initiated by adding 50 μL of the enzyme solution and monitored at 405 nm.

Human Cathepsin B.[24] Assay buffer was 100 mM sodium phosphate buffer, containing 100 mM NaCl, 5 mM EDTA and 0.01% Brij 35, pH 6.0. An enzyme stock solution of 1.81 mg/mL in 20 mM sodium acetate buffer containing 1 mM EDTA, pH 5.0, was diluted 1:500 with assay buffer containing 5 mM DTT and incubated for 30 min at 37 °C and kept at 0°C. A 100 mM stock solution of the chromogenic substrate Z-Arg-Arg-pNA was prepared with DMSO. The final concentrations were as follows: substrate, 500 μM (= 0.45 × K_m); DMSO, 2%; cathepsin B, 72 ng/mL. Into a cuvette containing 960 μL assay buffer, 15 μL inhibitor solution in DMSO and 5 μL of the substrate solution were added and thoroughly mixed. The reaction was performed at 37 °C, initiated by adding 20 μL of the enzyme solution and monitored at 405 nm.

Human Cathepsin L.[24] Assay buffer was 100 mM sodium phosphate buffer containing 100 mM NaCl, 5 mM EDTA and 0.01% Brij 35, pH 6.0. An enzyme stock solution of 135 μg/mL in 20 mM malonate buffer containing 400 mM NaCl and 1 mM EDTA, pH 5.5, was diluted 1:100 with assay buffer containing 5 mM DTT, incubated for 30 min at 37 °C and kept at 0°C. A 10 mM stock solution of the chromogenic substrate Z-Phe-Arg-pNA was prepared with DMSO. The final concentrations were as follows: substrate, 100 μM (= 5.88 × K_m); DMSO, 2%; cathepsin L, 54 ng/mL. Into a cuvette containing 940 μL assay buffer, 10 μL inhibitor solution in DMSO and 10 μL of the substrate solution were added and thoroughly mixed. The reaction was performed at 37 °C, initiated by adding 20 μL of the enzyme solution and monitored at 405 nm.

FRET Kinetics with Porcine Pancreatic Elastase. *λ_{ex} 320 nm FRET.* The reactions of probe **8** with PPE were followed by monitoring the fluorescence-resonance energy transfer from the anthranilic acid fluorophore to the coumarin 343 by setting the excitation wavelength for anthranilic acid at λ_{ex}= 320 nm and the emission wavelength of coumarin 343 at λ_{em} = 492 nm. A photomultiplier tube (PMT) value of 300 V was adjusted. The experiments were performed at

25°C for 60 min. Buffer was 50 mM sodium phosphate buffer and 500 mM NaCl, pH 7.8. A PPE solution was prepared in 10 mM sodium acetate buffer, pH 5.5. Probe **8** was dissolved DMSO. The final concentration of PPE was 3.1 U/mL and the final concentration of DMSO was 1.5%. Buffer, DMSO and probe **8** were placed in a cuvette. It was thoroughly mixed and the reaction was initiated by adding the enzyme. Experiments were performed in duplicate with five different inhibitor concentrations.

λ_{ex} 285 nm FRET. The experiments were performed as described above with the following exception. The reactions of **8** with PPE were followed over 60 min or 8 hours by monitoring a possible FRET from a tryptophan fluorophore of PPE to the coumarin 343 by setting the excitation wavelength for tryptophan at λ_{ex}= 285 nm and the emission wavelength of coumarin 343 at λ_{em} = 492 nm.

Detection of Human Neutrophil Elastase with the Activity-based Probe 8. *Estimation of the Detection Limit of the Probe.* A 200 µM solution of the activity-based probe **8** was prepared in DMSO. A HNE solution of 267 µg/mL was prepared in 100 mM sodium acetate buffer, pH 5.5. Elastase assay buffer (50 mM sodium phosphate buffer containing 500 mM NaCl, pH 7.8) was used to prepare mixtures of a total volume of 40 µL containing 2.5 µM of probe **8**, 2.5% DMSO and different concentration of HNE (11 ng/µL, 18 ng/µL, 25 ng/µL, 33 ng/µL, 40 ng/µL) (Fig. 5A). These mixtures were incubated at 25 °C for 20 min. To 18 µL of each mixture, 6 µL of reducing 4× Roti-Load 1 buffer (Roth, Karlsruhe, Germany) was added followed by heating at 95 °C for 5 min. After centrifugation (14,000 × *g*, 5 min), volumes of 20 µL were loaded and proteins were separated by SDS-PAGE. Gels (13%) were run in Tris/glycine/SDS buffer (Tris 25 mM, glycine 192 mM, SDS 0.1%). The enzyme was visualized by in-gel fluorescence detection using a Typhoon Trio scanner (GE Healthcare) and applying a setting which is most adequate for

the coumarin fluorophore, *i.e.* the 488-nm blue laser and an emission 520-nm band-pass filter (520 BP 40). A PMT value of 600 V and a pixel size scanning resolution of 100 µm were adjusted. Prestained marker proteins (PageRuler Plus Prestained Protein Ladder, ThermoFisher Scientific, Waltham, MA) served as standards.

Competition Experiment. A 400 µM solution of sivelestat (Sigma Aldrich, Germany) was prepared in DMSO. Two mixtures of a total volume of 39.5 µL containing HNE in both samples in the presence and absence of sivelestat in one sample were prepared in elastase assay buffer and incubated at 25 °C for 5 min. A volume of 0.5 µL of probe **8** was added to both samples to reach the following concentrations, 2.5 µM of probe **8**, 2.5% DMSO, 40 ng/µL of HNE and 5.0 µM of sivelestat. These mixtures were incubated at 25 °C for 20 min. SDS-PAGE and in-gel fluorescence detection (Fig. 5B) were performed as described above.

Survey of the Probe's Selectivity. Lysate from human embryonic kidney (HEK) 293 cells was received as described.[25] Four mixtures were prepared in elastase assay buffer, all containing probe **8**. A volume of 4.9 µL of HEK cell lysate, or 6.0 µL of HNE (twice), or 4.9 µL HEK cell lysate spiked with 6.0 µL of HNE were added. The mixtures were incubated at 25 °C for 20 min. After incubation, 4.9 µL of HEK cell lysate was added to one HNE sample. In the final volume of 40 µL, the mixtures contained 2.5 µM of probe **8**, 2.5% DMSO, 40 ng/µL of HNE and 0.60 µg/µL of HEK cell lysate. SDS-PAGE and in-gel fluorescence detection (Fig. 5C) were performed as described above.

Detection of endogenous HNE. Human granulocytes were isolated from peripheral blood of healthy donors using density gradient centrifugation (Histopaque, Sigma Aldrich). For the preparation of the cell lysates, purified granulocytes (40 mio cells) were lysed in 100 µL of lysis buffer (1% Triton X-100 in phosphate buffer saline, pH 7.4). Cell debris was removed by

centrifugation (12,000 *g*, 10 min). Two mixtures of a total volume of 19.75 µL containing cell lysate in both samples in the presence and absence of sivelestat were prepared in elastase assay buffer and incubated at 25 °C for 5 min. A volume of 0.25 µL of probe **8** was added to both samples to obtain the following concentrations, 2.5 µM of probe **8**, 2.5% DMSO, lysate of 6.12 mio cells and 5.0 µM of sivelestat. The mixtures were incubated at 25 °C for 20 min. SDS-PAGE and in-gel fluorescence detection (Fig. 6) were performed as described above.

Colloidal Coomassie G-250 Staining. Proteins were stained over night with PageBlue Protein Staining Solution (ThermoFisher Scientific, Waltham, MA). Gels were captured with a G:BOX F3 Gel Documentation System (Syngene, Cambridge, UK) using a visible light converter screen with the UV transilluminator (Figures 5D and 6B).

RESULTS AND DISCUSSION

Sulfonyloxyphthalimides have been reported as efficient inactivators for HNE and other serine proteases.[26-28] According to the mechanism depicted in Scheme 1,[26] the protease-inhibitor interaction involves a nucleophilic attack of the active-site serine residue at the carbonyl carbon leading to an opening of the heterocyclic ring and a subsequent Lossen rearrangement of the *O*-sulfonyl hydroxamic acid intermediate.[26,29,30] If the resulting isocyanate is trapped by water, the acyl enzyme undergoes slow hydrolysis and the enzymatic activity might be recovered. The isocyanate can alternatively react with a second, adjacent nucleophile from the protein matrix, *e.g.* with His-57 of HNE. In fact, the efficacy of such enzyme-activated inhibitors relies on the initially formed acyl enzyme, which keeps the isocyanate tethered at the active site and facilitates a second covalent attachment, leading to irreversible inactivation. This Lossen-based reactivity of low-molecular weight compounds bearing the cyclic CO-N(OSO_2Alk)-CO motif towards

serine proteases has also been shown for succinimides,[31,32] dihydrouracils,[33] and related heterocycles.[29] The mechanism of inactivation has been established by ^{13}C NMR studies,[31] and fluorescence spectroscopy.[26]

Scheme 1. Interaction between Sulfonyloxyphthalimides and Serine Proteases

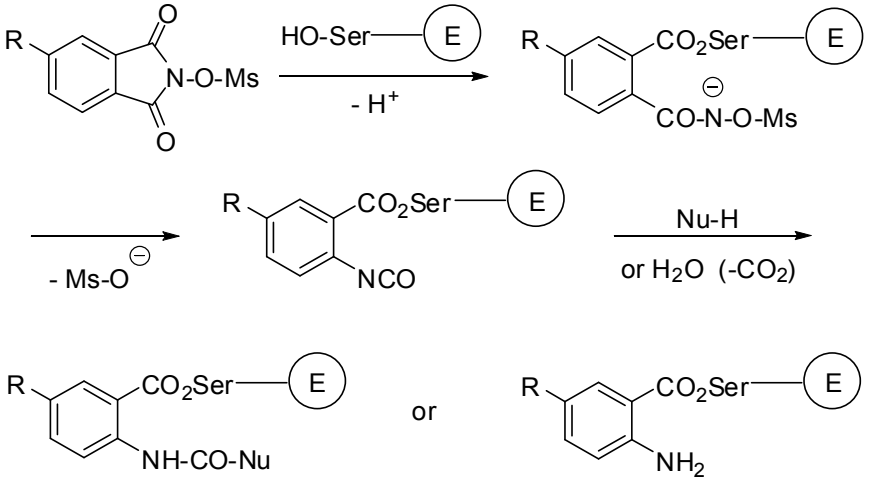

For the design of a new type of activity-based probes for HNE, we considered the formation of anthranilic acid derivatives (Scheme 1) in the course of the enzyme-inhibitor interaction. In order to devise a possible FRET sequence from the protein's tryptophan residues *via* anthranilic acid to a suitable fluorescent reporter, we decided to incorporate coumarin 343 into the ABP for HNE. Coumarins with donor groups at the position 7, such as coumarin 343, represent a widely used

class of fluorescent dyes. A small molecular size, high fluorescence quantum yields and large Stokes shifts, as well as chemical and enzymatic stability are their favored properties.[25,34]

We aimed at synthesizing a small series of linker-connected *N*-(mesyloxy)phthalimides (Scheme 2). The nitro-substituted *N*-hydroxyphthalimide **1** was chosen as the starting compound whose nitro group was reduced using Pd/C to afford compound **2**. This was converted into a sodium salt with $NaHCO_3$ and immediately reacted with methanesulfonyl chloride to obtain **3**.[35] A strong electrophile was required for a chemical modification of the aromatic amino group of **3**. After several unsuccessful attempts, the conversion of **3** was achieved with 4-nitrophenyl chloroformate. The resulting active carbamate **4** turned out to be readily suitable for the formation of a urea bridge to introduce different linker structures by a subsequent *in situ* coupling of **4** with various mono-Boc-protected diamines. Compounds **5a-d** either contain alkylidene or polyethylene glycol (PEG) linkers. These four intermediates were enzymatically evaluated and the most promising PEG derivative **5d** was selected for the generation of the final ABP. Removal of the Boc protecting group of **5d** under acidic conditions yielded **6**. This salt was coupled with coumarin 343 (**7**) in a HATU-promoted reaction to give the final probe **8** with coumarin 343 as fluorescence tag.

Scheme 2. Synthesis of Compound **8**[a]

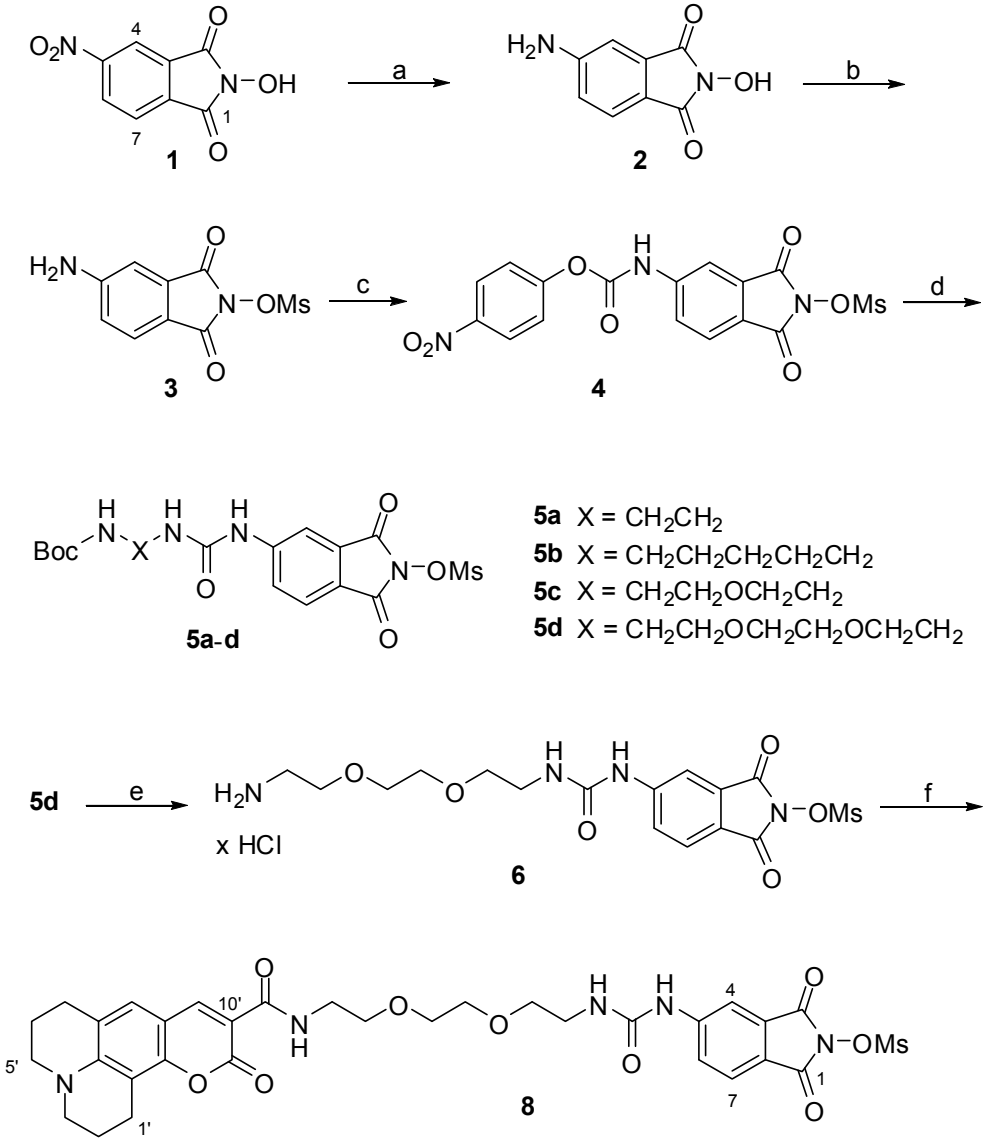

[a] Reactions and conditions: (a) H_2, Pd/C, CH_3OH, rt; (b) MsCl, $NaHCO_3$, H_2O, 0-5 °C; (c) 4-nitrophenyl chloroformate, THF, rt; (d) amine: Boc-NH-X-NH_2, DIPEA, rt; (e) 4N HCl in dioxane, CH_2Cl_2, rt, 2 h; (f) coumarin 343 (**7**), HATU, DIPEA, DMF, rt.

Compound **8** was investigated as an inhibitor of HNE by means of a spectroscopic assay with the chromogenic substrate MeOSuc-Ala-Ala-Pro-Val-pNA (Table 1). Additionally, an estimation of the bioactivity of the Boc-protected building blocks **5a-d** was carried out. These compounds showed time-dependent inhibition and the progress curves were analyzed with the slow-binding equation, implementing a distinct steady-state rate. From the first-order rate constants and the steady-rate rates, second-order rate constants for the formation of enzyme-inhibitor complexes, k_{on}, and K_i values, respectively, were obtained. The corresponding analysis for the HNE inhibition by probe **8** is depicted in Figure 1. The first-order rate constants for the decay of the enzyme-inhibitor complexes, k_{off}, were calculated from k_{on} and K_i values (Table 1). The kinetic parameters of the HNE inhibition by the five compounds do not differ much. From the k_{off} values, half-lives for the enzyme-inhibitor complexes between 56 min (**5d**) and 177 min (**5b**) were obtained. The K_i values were in the single-digit nanomolar range. As noted above, building block **5d** bearing a PEG linker with two oxygen atoms (PEG2) was selected as the precursor for the final ABP (**8**) because of similar enzyme-inhibiting activities of **5a-d**, and the envisaged improved water solubility of a PEG2-containing ABP. The exchange of the Boc-protecting group (in **5d**) by the coumarin 343 moiety (in **8**) did not result in a loss of inhibitory potency.

Table 1. Inhibition of HNE by Compounds **5a-d** and **8**[a]

Compound	K_i (nM)	k_{on} (10^4 $M^{-1}s^{-1}$)	$k_{off} = K_i\, k_{on}$ (10^{-4} s^{-1})
5a	6.83 ± 2.47	1.06 ± 0.15	0.726
5b	4.39 ± 1.63	1.49 ± 0.20	0.654
5c	6.81 ± 1.77	1.44 ± 0.57	0.981
5d	5.26 ± 1.00	3.91 ± 0.58	2.06
8	6.85 ± 0.39	2.37 ± 0.15	1.62

[a] Enzymatic activity was determined with five different inhibitor concentrations, [I], in duplicate measurements. Progress curves were analyzed using the slow-binding equation $[P] = v_s t + (v_i - v_s)(1-\exp(-k_{obs}t))/k_{obs} + d$, where [P] is the product concentration, v_s is the steady state rate, v_i is the initial rate, k_{obs} is the observed first-order rate constant and d is the offset. Values v_s were plotted *versus* inhibitor concentrations [I], and K_i values were obtained by non-linear regression according to $v_s = v_0/(1 + [I]/(K_i\,(1 + [S]/K_m))$, where v_0 is the rate in the absence of the inhibitor. The standard errors refer to this non-linear regression. The k_{on} values were obtained by linear regression according to $k_{obs} = [I]\, k_{on}\, /(1+ [S]/K_m) + k_{off}$. The standard errors refer to this linear regression.

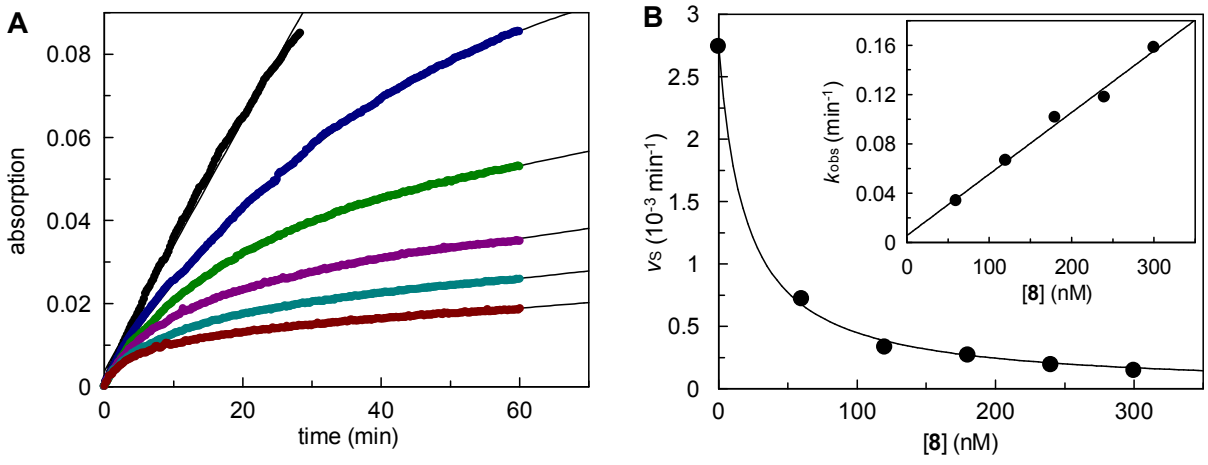

Figure 1. Inhibition of HNE by compound **8**. (A) The formation of *para*-nitroaniline from the chromogenic substrate MeOSuc-Ala-Ala-Pro-Val-pNA was recorded at 405 nm in the presence of different inhibitor concentrations (from top to bottom: 0 nM, 60 nM, 120 nM, 180 nM, 240 nM, 300 nM). Progress curves were analyzed by non-linear regression using the slow-binding equation $[P] = v_s t + (v_i - v_s)(1-\exp(-k_{obs}t))/k_{obs} + d$, where [P] is the product concentration, v_s is the steady-state rate, v_i is the initial rate, k_{obs} is the observed first-order rate constant, and d is the offset. (B) Steady-state rates v_s (mean values from duplicate measurements) were plotted *versus* the inhibitor concentrations. Inset: First-order rate constants k_{obs} (mean values from duplicate measurements) were plotted *versus* the inhibitor concentrations. The results are listed in Table 1.

ABP **8** was further evaluated using different serine and cysteine proteases, all of which are characterized by a covalent mode of catalysis. For this purpose, activity assays with chromogenic or fluorogenic peptide substrates were applied (Table 2). Compound **8** caused time-independent inhibition with linear progress curves in case of the human enzymes thrombin, cathepsin B and

cathepsin L as well as the bovine enzymes chymotrypsin, factor Xa and trypsin. In contrast, time-dependent inactivation was observed for HNE (see above) and porcine pancreatic elastase (PPE). In order to quote comparable values, half maximal inhibitory concentrations, corrected by the substrate concentration, are given in Table 2. These data indicate the strong preference of ABP **8** to inhibit the target enzyme HNE.

Table 2. Inhibition of Proteases by Probe **8**[a]

Protease	IC_{50} (1+ [S]/K_m)$^{-1}$ (μM)
HNE	0.0189 ± 0.0019
PPE	2.27 ± 0.30
chymotrypsin	6.48 ± 0.85
thrombin	5.87 ± 0.64
factor Xa	18.9 ± 1.0
trypsin	> 30
cathepsin B	9.49 ± 0.71
cathepsin L	0.353 ± 0.116

[a] Enzymatic activity was determined with five different inhibitor concentrations, [I], in duplicate measurements. The product formation within 60 min was used to determine v values, as rates of the reaction. IC_{50} values were obtained by non-linear regression using the equation $v = v_0/(1 + [I]/IC_{50})$, where v_0 is the rate in the absence and v the rate in the presence of the inhibitor. Values, corrected by the factor $(1 + [S]/K_m)$ are given. The standard errors refer to the non-linear regression.

The photophysical properties of ABP **8** were analyzed in three solvents, *i.e.* CH_2Cl_2, CH_3OH and H_2O (Fig. 2). The spectra of **8** exhibited slight bathochromic shifts for both absorption maxima and emission maxima with increasing polarity of the solvent and Stokes shifts between 34-44 nm. Thus, due to the properties of the coumarin 343 moiety, probe **8** appears to be qualified to act as the final fluorescence acceptor in FRET systems.

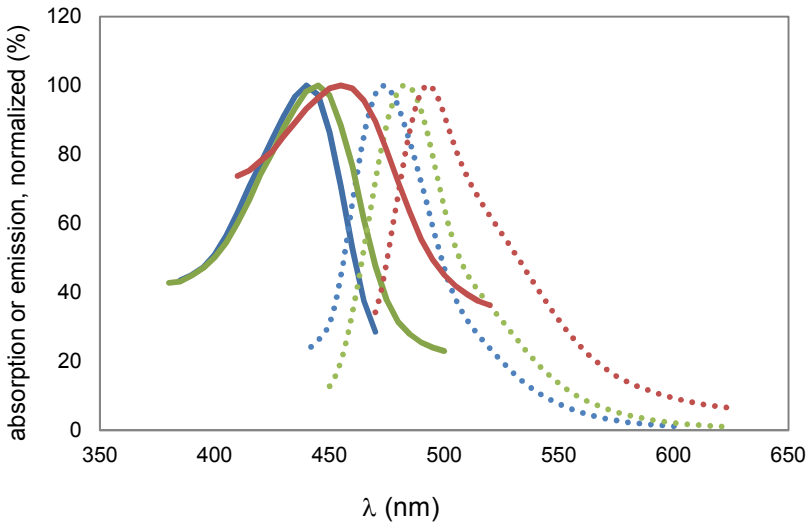

Figure 2. Absorption (5 µM, 1% DMSO, solid lines) and emission (1 µM, 1% DMSO, PMT value of 400 V, dotted lines) spectra of compound **8** recorded in H_2O (red lines), CH_3OH (green lines) and CH_2Cl_2 (blue lines), respectively. Absorption and emission maxima were as follows, λ_{ex} = 450 nm, λ_{em} = 492 nm (H_2O), λ_{ex} = 440 nm, λ_{em} = 484 nm (CH_3OH), λ_{ex} = 440 nm, λ_{em} = 474 nm (CH_2Cl_2).

To exploit a first FRET system, excessive PPE was incubated with ABP **8** at different concentrations and the reaction was followed over 60 min. Data of the first 33 min are shown in Figure 3. A wavelength of 320 nm was used for the excitation of anthranilic acid moieties which can function as the donor in an energy transfer process. The fluorescence kinetics was monitored with the emission wavelength of the coumarin 343 acceptor at 490 nm. The progress curves were analyzed by non-linear regression. In the absence of PPE, a gain in fluorescence was not observed for each ABP concentration (solid lines at the bottom of Fig. 3A). These findings clearly reflect the enzyme-catalyzed transformation of the probe. The formation of anthranilic acid derivative(s) was governed solely by the initial concentration of the probe **8** and the reactions obeyed a pseudo-first order kinetics. Accordingly, the initial rates linearly correlated with the concentration of the substrate, *i.e.* probe **8** (Fig. 3B). The product concentration at infinite time also depended on the initial concentration of **8**. In the course of the reaction, the fluorescence intensity approached constant values, which, however, might result from enzyme-bound and released anthranilic acid derivatives, both being capable to transfer energy to the coumarin acceptor. Although the surrounding environment of the anthranilic acid fluorophore changes upon hydrolysis, the constant fluorescence intensity indicate a similar behavior in the λ_{ex} 320 nm FRET system . As depicted in Scheme 3 and supported by the λ_{ex} 320 nm FRET experiment, ABP **8** interacts with PPE under ring opening and formation of the anthranoyl enzyme (**9**) which represents the covalently inhibited enzyme species. The consumption of **8** in this Lossen-type conversion is irreversible, but a fraction of the protease can recover its activity when **9** undergoes hydrolysis and the product of the enzyme-catalyzed conversion (**10**) is released.

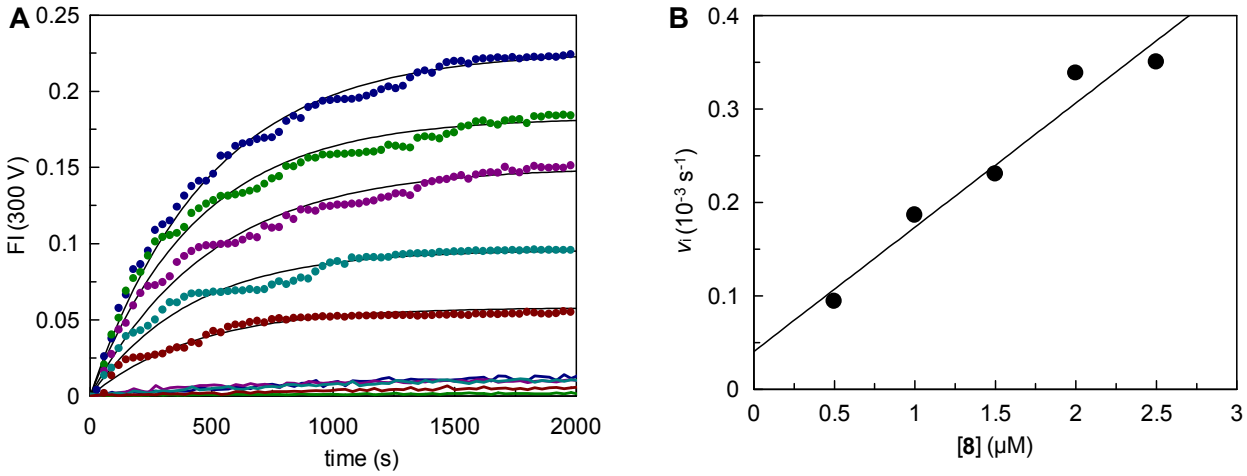

Figure 3. Fluorescence kinetics of the interaction of probe **8** with PPE. A λ_{ex} 320 nm FRET between two fluorophores was employed. The excitation of the anthranilic acid fluorophore at 320 nm led to an energy transfer to the coumarin fluorophore, whose emission was detected at 490 nm. (A) The progress curves over 33 min are shown. They were recorded in the presence of PPE (3.1 U/mL) and five different concentrations of **8**, from top to bottom: 2.5 μM, 2.0 μM, 1.5 μM, 1.0 μM, 0.5 μM. Reactions in the absence of PPE are shown as solid lines. Progress curves over 60 min were analyzed using the exponential equation $FI = v_i\,(1-\exp(-k_{obs}t))/k_{obs} + d$, where FI is the fluorescence intensity as generated by the λ_{ex} 320 nm FRET, v_i is the initial rate, k_{obs} is the observed first-order rate constant and d is the offset. (B) The values v_i (means of two independent experiments) were plotted versus concentrations of probe **8**.

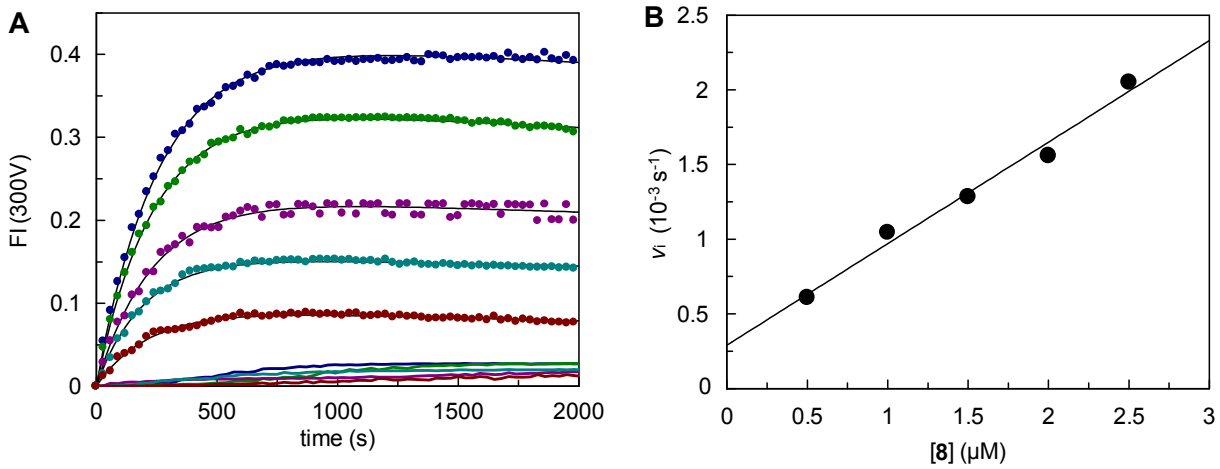

Figure 4. Fluorescence kinetics of the interaction of probe **8** with PPE. A λ_{ex} 285 nm FRET between three fluorophores was assumed. An excitation of the tryptophan fluorophore of PPE at 285 nm would lead to the first, hypothesized energy transfer from tryptophan to the second, anthranilic acid fluorophore. Its excitation produced the second energy transfer to the coumarin fluorophore, whose emission was detected at 490 nm. (A) The progress curves over 33 min are shown. They were recorded in the presence of PPE (3.1 U/mL) and five different concentrations of **8**, from top to bottom: 2.5 μM, 2.0 μM, 1.5 μM, 1.0 μM, 0.5 μM. Reactions in the absence of PPE are shown as solid lines. Progress curves over 60 min were analyzed using the slow-binding equation $FI = v_s t + (v_i - v_s)(1-\exp(-k_{obs}t))/k_{obs} + d$, where FI is the fluorescence intensity as generated by the λ_{ex} 285 nm FRET, v_s is the steady state rate, v_i is the initial rate, k_{obs} is the observed first-order rate constant and d is the offset. (B) The values v_i (means of two independent experiments) were plotted versus concentrations of probe **8**.

Scheme 3. Assumed FRET Systems to Study the Interaction of Probe **8** with Elastase[a]

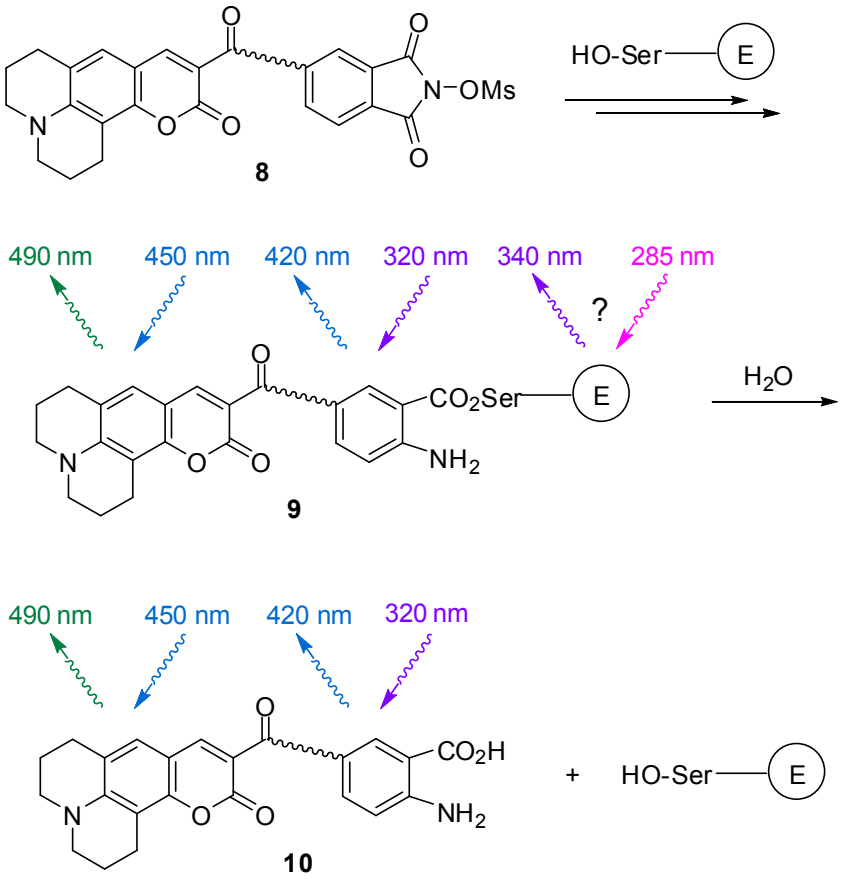

[a] A supposed λ_{ex} 285 nm FRET between the enzyme's tryptophan (excitation 285 nm) and coumarin 343 (emission 490 nm). A λ_{ex} 320 nm FRET between the anthranilic acid moiety (excitation 320 nm) and coumarin 343 (emission 490 nm).

Next, it was intended to comprise the tryptophan fluorescence of PPE. For the generation of a FRET signal, there are two tryptophan residues in a sufficient distance to the active site.[36] These distances of about 11-12 Å were estimated by building a model of a covalent complex, see Supporting Information (SI, Fig. S1). For this purpose, we have modeled the active site of PPE

with the catalytic serine residue bound to an unsubstituted anthranoyl residue, representing a simplified model of complex **9** (Scheme 3). The phenyl ring of the resulting Ser195-anthranilic acid ester complex acts as a fluorophore that can be excited by the nearby tryptophan moieties.

The following FRET kinetic experiments have been designed to include the excitation of tryptophan at 285 nm, which, in turn, might excite the anthranilic acid fluorophore, leading to the excitation of the coumarin moiety and the emission at 490 nm (Scheme 3). Except of the excitation wavelength, the λ_{ex} 285 nm FRET experiment was performed under the same conditions as described above. We monitored a strong increase in fluorescence intensity within the first 15 min, which expectedly depended on the initial concentration of the probe **8** (Fig. 4A). A slow decrease in fluorescence intensity at the later stage of the reaction was observed. Accordingly, an equation for the non-linear regression of the progress curves was used which includes final slopes different from zero. The pseudo-first order kinetics was confirmed also for this process by demonstrating the linear correlation between the initial rates and the concentrations of probe **8** as shown in the corresponding secondary plot (Fig. 4B).

The λ_{ex} 285 nm FRET setup provided experimental support for the formation of an enzyme-probe complex which contains the anthranilic acid fluorophore (*i.e.* complex **9**, Scheme 3). The modified probe **10** was probably not recorded due to the interruption of the FRET system when complex **9** dissociated. Thus, the slow hydrolytic cleavage of **9** was supposed to account for the late decrease of the fluorescence signal. In a separate experiment, fluorescence kinetics was followed over 8 hours by applying the same λ_{ex} 285 nm FRET setup. After reaching maximal fluorescence intensity, an exponential decrease was observed. The progress curves of this later stage were monitored and analyzed with the equation of the exponential decay, see Supporting Information (SI, Fig. S2). The half-live of the anthranoyl enzyme **9** which is capable of

producing the λ_{ex} 285 nm FRET was estimated to be 3.3 hours. This value, obtained by fluorescence kinetics with PPE, is in the same range as the half-live of 71 min as obtained from inhibition kinetics with HNE. The difference is assumed to be mainly due to the origin of the enzyme in both experiments. The decay of this complex **9** indicates the involvement of tryptophan residue(s) in the first energy transfer step. These assumption is furthermore supported by afore-described inhibition kinetics with mesyloxyphthalimides which showed steady-state rates different from zero, again reflecting a slow release of the ring-opened probe and the simultaneous recovery of the protease. However, further experimental evidence is needed to clarify the involvement of tryptophan(s) in the λ_{ex} 285 nm FRET system. For example, in future studies, the FRET efficiency might be examined with the enzyme mutated on the two tryptophan residues in proximity to the active site.

The suitability of compound **8** as an activity-based probe was proved by in-gel fluorescence analysis of HNE (Fig. 5). HNE at different concentrations was treated with 2.5 μM of **8** for 20 min. Following SDS-PAGE, fluorescent bands at approximately 29 kDa could be detected and amounts as low as 160 ng of HNE successfully visualized (lanes 1-5 in Fig. 5A). Three bands were observed for HNE (*e.g.* lane 2 in Fig. 5B, lane 2-3 in Fig. 5C). It is known that several HNE isoforms can be resolved by SDS-PAGE and that these catalytically active forms only differ in their carbohydrate content. Moreover, the self-cleavage of elastase from murine and human neutrophils was shown to generate variants of different catalytic activity.[37] Since elastase used in our study was prepared from human neutrophils, we assume that the three bands correspond to HNE isoforms with different glycosylation patterns or are caused by autocatalytic cleavage.

The binding mode of probe **8** in the active site of HNE was verified by a competition experiment (Fig. 5B). HNE was incubated for 5 min with 5 μM of the active-site directed,

covalent inhibitor sivelestat,[4] followed by 2.5 μM of ABP **8** (lane 1 in Fig. 5B). In the control experiment, HNE was incubated with DMSO prior to the addition of the probe (lane 2 in Fig. 5B). Sivelestat was able to protect HNE from a reaction with the probe as the detectable fluorescence at ~29 kDa was strongly reduced. These findings confirmed the active-site directed interaction of **8** with HNE and indicated that surface nucleophiles of the enzyme were obviously not affected by probe **8**.

Furthermore, the selectivity of HNE labeling by **8** was studied as illustrated in Figures 5C and 5D. HEK293 cell lysate was spiked with HNE, incubated with the probe, subjected to SDS-PAGE and analyzed by fluorescence imaging. In contrast to the imaging of 600 ng of HNE (lane 2 in Fig. 5C), amounts of 9 μg HEK cell lysate protein did not produce fluorescent bands (lane 1 in Fig. 5C), indicating that **8** did not react with non-target proteins. As a control, the gel was subsequently stained with Coomassie blue (lanes 1 and 2 in Fig. 5D). We performed two spiking experiments (lanes 3 and 4 in Figures 5C and 5D). HEK lysate was added either after the incubation to the mixture of HNE and **8**, or prior to the incubation. When HNE was incubated with **8** only, the protease has been inactivated due to reaction with **8** and, thus, became unable to degrade the lysate's proteins. Therefore, the Coomassie staining of the protein mixtures in lanes 1 and 3 (Fig. 5D) was similar. However, when HNE was simultaneously incubated with the lysate and **8**, protein degradation occurred and the enzyme was partly protected from being inactivated by **8** due to the consumption of protein substrates. This led to a different protein pattern (lane 4 *versus* lane 3 in Fig. 5D) and to a slightly reduced intensity of the fluorescent signal of HNE (lane 4 *versus* lane 3 in Fig. 5C). Importantly, this analysis revealed selective labeling of the target HNE within a mixture of excess proteins without detectable nonspecific interactions of **8** (lanes 3 and 4 in Fig. 5C).

Therefore, in the course of this study, we thought to assess the suitability of ABP **8** for detecting endogenous elastase. For this purpose, neutrophil granulocytes from human donors were purified by density gradient centrifugation and lysates were prepared by detergent (Triton X-100) treatment. The following analysis by gel electrophoresis of the lysate proteome revealed a fluorescent band at ~29 kDa which could clearly be assigned to HNE (lane 3 in Fig. 6A). In the competition experiment, it was shown, that the addition of sivelestat prior to the probe **8** was able to abolish HNE labeling (lane 2 in Fig. 6A), again indicating that both, probe **8** and sivelestat, target the active site of HNE. The Coomassie blue staining (lanes 1-3 in Fig. 6B) indicated that the endogenous amount of HNE was not particularly prominent in the lysate. Thus, this in-lysate experiment even more accentuated the strong labeling capability of our activity-based probe.

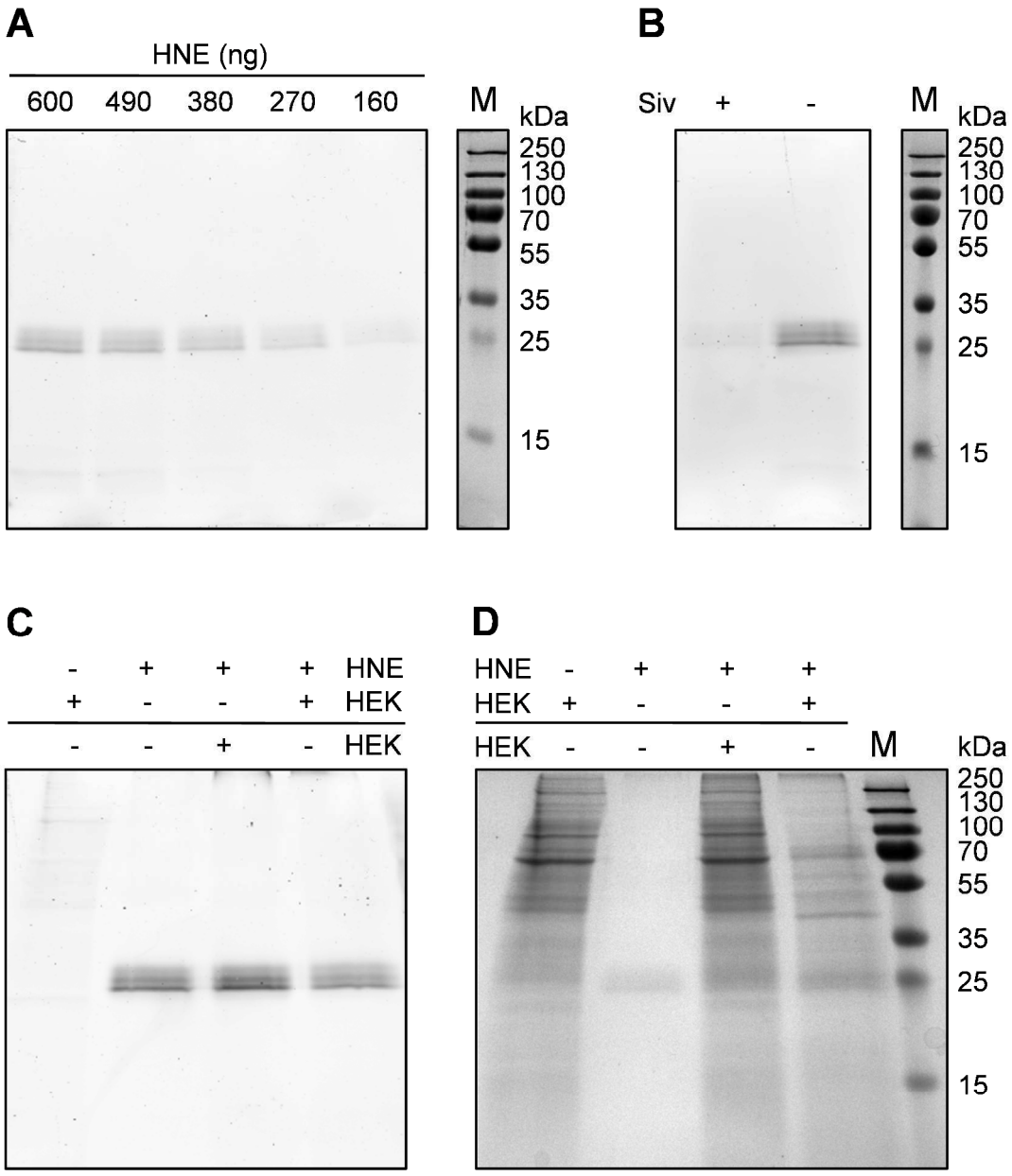

Figure 5. Imaging of HNE with the fluorescent probe **8**. (A) HNE in different concentrations (11 – 40 ng/μL) was incubated with 2.5 μM of **8** for 20 min at 25 °C. The mixtures were subjected to reducing SDS-PAGE. The amounts of HNE applied to individual lanes are indicated. (B) HNE (40 ng/μL) was preincubated in the presence or absence of 5 μM of sivelestat (Siv) for 5 min at 25 °C. Probe **8** (2.5 μM) was added, the mixtures were incubated for further 20 min at 25 °C and

subjected to reducing SDS-PAGE. (C) Lanes 1 and 2: HEK cell lysate (0.60 μg/μL) or HNE (40 ng/μL) were incubated for 20 min at 25 °C in the presence of 2.5 μM of **8** and subjected to reducing SDS-PAGE. Lanes 3 and 4: HNE (40 ng/μL) was incubated for 20 min at 25 °C in the presence of 2.5 μM of **8** and HEK lysate (0.60 μg/μL) was added after the incubation. A mixture HNE (40 ng/μL) and HEK lysate (0.60 μg/μL) were incubated in the presence of 2.5 μM of **8**. Both mixtures were subjected to reducing SDS-PAGE. (D) After SDS-PAGE described in (C), the proteins in were visualized by Coomassie staining. (A-D) M, molecular mass marker.

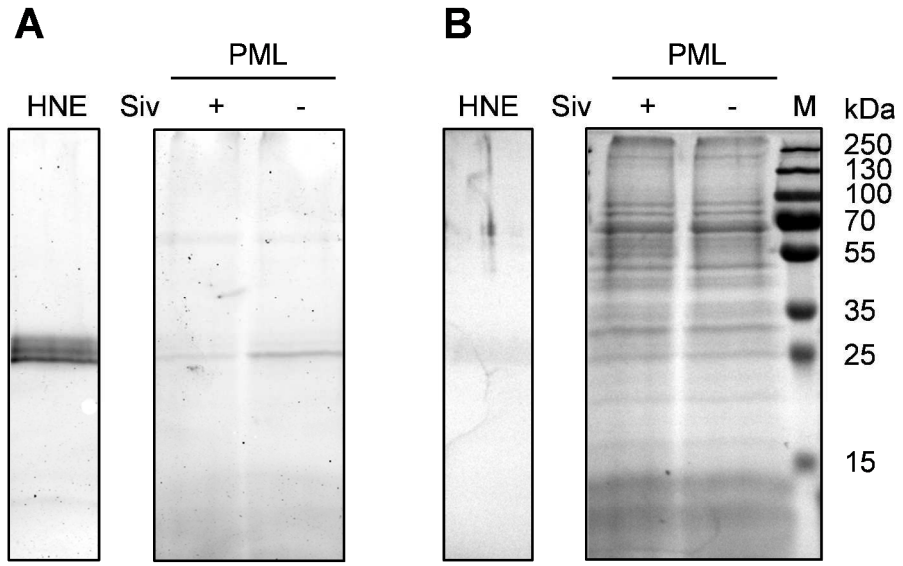

Figure 6. Imaging of endogenous HNE with probe **8**. (A) HNE (40 ng/μL) and lysate of human polymorphonuclear leukocytes (PML), in the presence or absence of 5 μM of sivelestat (Siv), were incubated with 2.5 μM of **8** for 20 min at 25 °C. The mixtures were subjected to reducing SDS-PAGE. (B) After SDS-PAGE, the proteins in were visualized by Coomassie staining. M, molecular mass marker.

CONCLUSIONS

In conclusion, we have developed a novel fluorescent probe for human neutrophil elastase. For the chemical design, a phthalimide precursor for a Lossen rearrangement was chosen. The Lossen rearrangement to functionalized isocyanates gives rise to a variety of inter- and intramolecular transformations. While it has accordingly been applied to manifold preparative purposes, its application for activity-based probing has been reported herein for the first time. In the fluorescence kinetic experiments, two FRET systems (λ_{ex} 320 nm FRET and λ_{ex} 285 nm FRET) were employed and it was shown that the observed fluorescence transfers exclusively arose from the interaction of the ABP with the target protease. The applicability of the probe was demonstrated by in-gel fluorescent detection analyses. Our probe was capable to visualize endogenous elastase from human neutrophils. The activity-based probe is expected to serve as a valuable tool compound for future investigations of elastase, a therapeutically relevant protease, and neutrophil-mediated proteolytic events.

ASSOCIATED CONTENT

Supporting Information. Covalent docking experiments, a λ_{ex} 285 nm FRET experiment, all synthetic procedures, ^{1}H and ^{13}C NMR spectra of newly synthesized compounds.

AUTHOR INFORMATION

Corresponding Author

Pharmaceutical Institute, Pharmaceutical Chemistry I, An der Immenburg 4, D-53121 Bonn, Germany. Phone: +49-228-732317. Fax: +49-228-732567. E-mail: guetschow@uni-bonn.de

Author Contributions

M.G. conceived the study. A.C.S.F., A.S.T., A.B., T.G. and E.G. performed experiments. All authors analyzed data. A.C.S.F., A.B., J.B., S.N. and M.G. wrote the manuscript.

ACKNOWLEDGMENT

A.S.F. was supported by a fellowship from the DAAD (IPID4all program). The authors thank Marit Stirnberg, Anna-Madeleine Beckmann and Martin Mangold for providing cell lysates, Oscar M. Bautista-Aguilera for synthetic support and Anke Gühler for technical assistance.

ABBREVIATIONS

ABP, activity-based probe; ALI, acute lung injury; ARDS, acute respiratory distress syndrome; DAD, diode array detection; DIPEA, diisopropylethylamine; FRET, Förster resonance energy transfer; HATU, *O*-(7-azabenzotriazol-1-yl)-*N*,*N*,*N*′,*N*′-tetramethyluronium-hexafluorphosphat; HEK, human embryonic kidney; HNE, human neutrophil elastase; LTB_4, leukotriene B_4; PEG, polyethylene glycol; PMT, photomultiplier tube; pNA, *para*-nitroanilide; PPE, porcine pancreatic elastase; siv, sivelestat.

REFERENCES

(1a) Korkmaz, B., Moreau, T., and Gauthier, F. (2008) Neutrophil elastase, proteinase 3 and cathepsin G: physicochemical properties, activity and physiopathological functions. *Biochimie 90*, 227–242. (b) Korkmaz, B., Horwitz, M. S., Jenne, D. E., and Gauthier, F. (2010) Neutrophil elastase, proteinase 3, and cathepsin G as therapeutic targets in human diseases. *Pharmacol. Rev. 62*, 726–759. (c) Lucas, S. D., Costa, E., Guedes, R. C., and Moreira, R. (2013) Targeting COPD: advances on low-molecular-weight inhibitors of human neutrophil elastase. *Med. Res. Rev.* E73–101. (d) von Nussbaum, F., and Li, V. M. (2015) Neutrophil elastase inhibitors for the treatment of (cardio)pulmonary diseases: Into clinical testing with pre-adaptive pharmacophores. *Bioorg. Med. Chem. Lett. 25*, 4370–4381.

(2) Brinkmann, V., Reichard, U., Goosmann, C., Fauler, B., Uhlemann, Y., Weiss, D. S., Weinrauch, Y., and Zychlinsky, A. (2004) Neutrophil extracellular traps kill bacteria. *Science 303*, 1532–1535.

(3a) Young, R. E.; Voisin, M. B.; Wang, S., Dangerfield, J., and Nourhsargh, S. (2007) Role of neutrophil elastase in LTB4-induced neutrophil transmigration in vivo assessed with a specific inhibitor and neutrophil elastase deficient mice. *Br. J. Pharmacology 151*, 628–637. (b) Colom, B., Bodkin, J. V., Beyrau, M., Woodfin, A., Ody, C., Rourke, C., Chavakis, T., Brohi, K., Imhof, B. A., and Nourshargh, S. (2015) Leukotriene B_4-neutrophil elastase axis drives neutrophil reverse transendothelial cell migration in vivo. *Immunity 42*, 1075–1086. (c) Reglero-Real, N., Colom, B., Bodkin, J. V., and Nourshargh, S. (2016) Endothelial cell junctional adhesion molecules: role and regulation of expression in inflammation. *Arterioscler. Thromb. Vasc. Biol. 36*, 2048–2057.

(4a) Kawabata, K., Suzuki, M., Sugitani, M., Imaki, K., Toda, M., and Miyamoto, T. (1991) ONO-5046, a novel inhibitor of human neutrophil elastase. *Biochem. Biophys. Res. Commun. 177*, 814–820. (b) Nakayama, Y., Odagaki, Y., Fujita, S., Matsuoka, S., Hamanaka, N., Nakai, H., and Toda, M. (2002) Clarification of mechanism of human sputum elastase inhibition by a new inhibitor, ONO-5046, using electrospray ionization mass spectrometry. *Bioorg. Med. Chem. Lett. 12*, 2349–2353.

(5) Winiarski, Ł., Oleksyszyn, J., and Sieńczyk, M. (2012) Human neutrophil elastase phosphonic inhibitors with improved potency of action. *J. Med. Chem. 55*, 6541−6553.

(6) Krantz, A., Spencer, R. W., Tam, T. F., Thomas, E., and Copp, L. J. (1987) Design of alternate substrate inhibitors of serine proteases. Synergistic use of alkyl substitution to impede enzyme-catalyzed deacylation. *J. Med. Chem. 30*, 489−491.

(7a) Mulchande, J.; Guedes, R. C.; Tsang, W. Y.; Page, M. I.; Moreira, R.; and Iley, J. (2008) Azetidine-2,4-diones (4-oxo-beta-lactams) as scaffolds for designing elastase inhibitors. *J. Med. Chem. 51*, 1783−1790. (b) Mulchande, J.; Oliveira, R., Carrasco, M., Gouveia, L., Guedes, R. C.,

Iley, J., and Moreira, R. (2010) 4-Oxo-beta-lactams (azetidine-2,4-diones) are potent and selective inhibitors of human leukocyte elastase. *J. Med. Chem. 53*, 241−253. (c) Groutas, W. C., Houser-Archield, N., Chong, L. S., Venkataraman, R., Epp, J. B., Huang, H., and McClenahan, J. J. (1993) Efficient inhibition of human leukocyte elastase and cathepsin G by saccharin derivatives. *J. Med. Chem. 36*, 3178−3181.

(8) Lucas, S. D., Gonçalves, L. M., Carvalho, L. A., Correia, H. F., Da Costa, E. M., Guedes, R. A., Moreira, R., and Guedes, R. C. (2013) Optimization of O3-acyl kojic acid derivatives as potent and selective human neutrophil elastase inhibitors. *J. Med. Chem. 56*, 9802−9806.

(9) Köcher, S., Rey, J., Bongard, J., Tiaden, A. N., Meltzer, M., Richards, P. J., Ehrmann, M., and Kaiser, M. (2017) Tailored Ahp-cyclodepsipeptides as potent non-covalent serine protease inhibitors. *Angew. Chem. Int. Ed. 56*, 8555−8558.

(10a) Patel, N., Belcher, J., Thorpe, G., Forsyth, N. R., and Spiteri, M. A. (2015) Measurement of C-reactive protein, procalcitonin and neutrophil elastase in saliva of COPD patients and healthy controls: Correlation to self-reported wellbeing parameters. *Respir. Res.* 16:62. (b) Chalmers, J. D., Moffitt, K. L., Suarez-Cuartin, G., Sibila, O., Finch, S., Furrie, E., Dicker, A., Wrobel, K., Elborn, J. S., Walker, B., Martin, S. L., Marshall, S. E., Huang, J. T., and Fardon, T. C. (2017) Neutrophil elastase activity is associated with exacerbations and lung function decline in bronchiectasis. *Am. J. Respir. Crit. Care Med. 195*, 1384−1393. (c) Bihlet, A. R., Karsdal, M. A., Sand, J. M., Leeming, D. J., Roberts, M., White, W., and Bowler, R. (2017) Biomarkers of extracellular matrix turnover are associated with emphysema and eosinophilic-bronchitis in COPD. *Respir. Res.* 18:22.

(11a) Sabidó, E., Tarragó, T., Niessen, S., Cravatt, B. F., and Giralt, E. (2009) Activity-based probes for monitoring postproline protease activity. *ChemBioChem 10*, 2361–2366. (b) Sabidó,

E., Tarragó, T., and Giralt, E. (2010) Towards the identification of unknown neuropeptide precursor-processing enzymes: Design and synthesis of a new family of dipeptidyl phosphonate activity probes for substrate-based protease identification. *Bioorg. Med. Chem. 18*, 8350–8355. (c) Sanman, L. E., and Bogyo, M. (2014) Activity-Based Profiling of Proteases. *Annu. Rev. Biochem. 83*, 249–273. (d) Willems, L. I., Overkleeft, H. S., and van Kasteren, S. I. (2014) Current developments in Activity-Based Protein Profiling. *Bioconjugate Chem. 25*, 1181−1191. (e) de Bruin, G., Xin, B. T., Kraus, M., van der Stelt, M., van der Marel, G. A., Kisselev, A. F., Driessen, C., Florea, B. I., and Overkleeft, H. S.(2016) A set of activity-based probes to visualize human (immuno)proteasome activities. *Angew. Chem. Int. Ed. Engl. 55*, 4199−4203. (f) van Kasteren, S. I., Florea, B. I., and Overkleeft, H. S. (2017) Activity-based protein profiling: From chemical novelty to biomedical stalwart. *Methods Mol. Biol.* 1491:1–8. (g) Zweerink, S., Kallnik, V., Ninck, S., Nickel, S., Verheyen, J., Blum, M., Wagner, A., Feldmann, I., Sickmann, A., Albers, S. V., Bräsen, C., Kaschani, F., Siebers, B., and Kaiser, M. (2017) Activity-based protein profiling as a robust method for enzyme identification and screening in extremophilic Archaea. *Nat. Commun.* 8:15352.

(12) Haedke, U., Götz, M., Baer, P., and Verhelst, S. H. (2012) Alkyne derivatives of isocoumarins as clickable activity-based probes for serine proteases. *Bioorg. Med. Chem. 20*, 633−640.

(13) Shannon, D. A., Gu, C., McLaughlin, C. J., Kaiser, M., van der Hoorn, R. A., and Weerapana, E. (2012) Sulfonyl fluoride analogues as activity-based probes for serine proteases. *ChemBioChem 13*, 2327−2330.

(14) Ruivo, E. F., Gonçalves, L. M., Carvalho, L. A., Guedes, R. C., Hofbauer, S., Brito, J. A., Archer, M., Moreira, R., and Lucas, S. D. (2016) Clickable 4-oxo-β-lactam-based selective probing for human neutrophil elastase related proteomes. *ChemMedChem 11*, 2037−2042.

(15a) Serim, S., Mayer, S. V., and Verhelst, S. H. (2013) Tuning activity-based probe selectivity for serine proteases by on-resin "click" construction of peptide diphenyl phosphonates. *Org. Biomol. Chem. 11*, 5714–5721. (b) Lechtenberg, B. C., Kasperkiewicz, P., Robinson, H., Drag, M., and Riedl, S. J. (2015) The elastase-PK101 structure: mechanism of an ultrasensitive activity-based probe revealed. *ACS Chem. Biol. 10*, 945−951.

(16a) Gehrig, S., Mall, M. A., and Schultz, C. (2012) Spatially resolved monitoring of neutrophil elastase activity with ratiometric fluorescent reporters. *Angew. Chem. Int. Ed. 51*, 6258–6261. (b) de Bruin, G., Xin, B. T., Florea, B. I., and Overkleeft, H. S. (2016) Proteasome subunit selective activity-based probes report on proteasome core particle composition in a native polyacrylamide gel electrophoresis fluorescence-resonance energy transfer assay. *J. Am. Chem. Soc. 138*, 9874–9880. (c) Okamoto, K., and Sako, Y. (2017) Recent advances in FRET for the study of protein interactions and dynamics. *Curr. Opin. Struct. Biol. 46*, 16–23. (d) Bunt, G., and Wouters, F. S. (2017) FRET from single to multiplexed signaling events. *Biophys. Rev.* 9, 119–129.

(17) Gütschow, M., Pietsch, M., Themann, A., Fahrig, J., and Schulze, B. (2005) 2,4,5-Triphenylisothiazol-3(2*H*)-one 1,1-dioxides as inhibitors of human leukocyte elastase. *J. Enzyme Inhib. Med. Chem. 20*, 341–347.

(18) Castillo, M. J., Nakajima, K., Zimmerman, M., and Powers, J. C. (1979) Sensitive substrates for human leukocyte and porcine pancreatic elastase: a study of the merits of various

chromophoric and fluorogenic leaving groups in assays for serine proteases. *Anal. Biochem. 99*, 53–64.

(19) Neumann, U., and Gütschow, M. (1995) 3,1-Benzothiazin-4-ones and 3,1-benzoxazin-4-ones: Highly different activities in chymotrypsin inactivation. *Bioorg. Chem. 23*, 72–88.

(20) Steinebach, C., Schulz-Fincke, A. C., Schnakenburg, G., and Gütschow, M. (2016) In situ generation and trapping of thioimidates: An intermolecular tandem reaction to 4-acylimino-4*H*-3,1-benzothiazines. *RSC Advances 6*, 15430–15440.

(21) Dosa, S., Stirnberg, M., Lülsdorff, V., Häußler, D., Maurer, E., and Gütschow, M. (2012) Active site mapping of trypsin, thrombin and matriptase-2 by sulfamoyl benzamidines. *Bioorg. Med. Chem. 20*, 6489–6505.

(22) Häußler, D., Scheidt, T., Stirnberg, M., Steinmetzer, T., and Gütschow, M. (2015) A Bisbenzamidine phosphonate as a Janus-faced inhibitor for trypsin-like serine proteases. *ChemMedChem 10*, 1641–1646.

(23) Sisay, M. T., Steinmetzer, T., Stirnberg, M., Maurer, E., Hammami, M., Bajorath, J., and Gütschow, M. (2010) Identification of the first low-molecular-weight inhibitors of matriptase-2. *J. Med. Chem. 53,* 5523–5535.

(24) Frizler, M., Lohr, F., Lülsdorff, M., and Gütschow, M. (2011) Facing the gem-dialkyl effect in enzyme inhibitor design: preparation of homocycloleucine-based azadipeptide nitriles. *Chem. Eur. J. 17*, 11419–11423.

(25) Häußler, D., Schulz-Fincke, A. C., Beckmann, A. M., Keils, A., Gilberg, E., Mangold, M., Bajorath, J., Stirnberg, M., Steinmetzer, T.; and Gütschow, M. (2017) A fluorescent-labeled phosphono bisbenzguanidine as an activity-based probe for matriptase. *Chem. Eur. J. 23*, 5205–5209.

(26) Neumann, U., and Gütschow, M. (1994) *N*-(Sulfonyloxy)phthalimides and analogs are potent inactivators of serine proteases. *J. Biol. Chem. 269*, 21561–21567.

(27) Kerrigan, J. E., Walters, M. C., Forrester, K. J., Crowder, J. B., and Christopher, L. J. (2000) 6-Acylamino-2-[(alkylsulfonyl)oxy]-1*H*-isoindole-1,3-dione mechanism-based inhibitors of human leukocyte elastase. *Bioorg. Med. Chem. Lett. 10*, 27–30.

(28) Vagnoni, L. M., Gronostaj, M., and Kerrigan, J. E. (2001) 6-Acylamino-2-1[(ethylsulfonyl)oxy]-1*H*-isoindole-1,3-diones mechanism-based inhibitors of human leukocyte elastase and cathepsin G: Effect of chirality in the 6-acylamino substituent on inhibitory potency and selectivity. *Bioorg. Med. Chem*. *9*, 637–645.

(29) Martyn, D. C., Moore, M. J., and Abell, A. D. (1999) Succinimide and saccharin-based enzyme-activated inhibitors of serine proteases. *Curr. Pharm. Des.* 5, 405−415.

(30) Gütschow, M. (1999) One-pot reactions of *N*-(mesyloxy)phthalimides with secondary amines to 2-ureidobenzamides, 2-ureidobenzoic acids, ethyl 2-ureidobenzoates, or isatoic anhydrides. *J. Org. Chem. 64*, 5109–5115.

(31) Groutas, W. C., Stanga, M. A., and Brubaker, M. J. (1989) ^{13}C NMR evidence for an enzyme-induced Lossen rearrangement in the mechanism-based inactivation of alpha-chymotrypsin by 3-benzyl-*N*-((methylsulfonyl)oxy)succinimide. *J. Am. Chem. Soc. 111*, 1931–1932.

(32a) Groutas, W. C., Brubaker, M. J., Venkataraman, R., and Stanga, M. A. (1992) Enantioselective inhibition of human leukocyte elastase. *Arch. Biochem. Biophys. 297,* 144−146. (b) Abell, A. D., Oldham, M. D. (1999) Leucine-phenylalanine dipeptide-based *N*-mesyloxysuccinimides: synthesis of all four stereoisomers and their assay against serine proteases. *Bioorg. Med. Chem. Lett. 9*, 497−500.

(33) Groutas, W. C., Huang, H., Epp, J. B., Brubaker, M. J., Keller, C. E., and McClenahan, J. J. (1992) A general approach toward the design of inhibitors of serine proteinases: Inhibition of human leukocyte elastase by substituted dihydrouracils. *Bioorg. Med. Chem. Lett. 2*, 1565−1570.

(34a) Agnes, R. S., Jernigan, F., Shell, J. R., Sharma, V., and Lawrence, D. S. (2010) Suborganelle sensing of mitochondrial cAMP-dependent protein kinase activity. *J. Am. Chem. Soc. 132*, 6075–6080. (b) Nizamov, S., Willig, K. I., Sednev, M. V., Belov, V. N., and Hell, S. W. (2012) Phosphorylated 3-heteroarylcoumarins and their use in fluorescence microscopy and nanoscopy. *Chem. Eur. J. 18*, 16339–16348. (c) Mertens, M. D., Schmitz, J., Horn, M., Furtmann, N., Bajorath, J., Mareš, M., and Gütschow, M. (2014) A coumarin-labeled vinyl sulfone as tripeptidomimetic activity-based probe for cysteine cathepsins. *ChemBioChem 15*, 955–959. (d) Häußler, D., Mangold, M., Furtmann, N., Braune, A., Blaut, M., Bajorath, J., Stirnberg, M., and Gütschow, M. (2016) Phosphono bisbenzguanidines as irreversible dipeptidomimetic inhibitors and activity-based probes of matriptase-2. *Chem. Eur. J. 22*, 8525–8535. (e) Cottam Jones, J. M., Harris, P. W., Scanlon, D. B., Forbes, B. E., Brimble, M. A., and Abell, A. D. (2016) Fluorescent IGF-II analogs for FRET-based investigations into the binding of IGF-II to the IGF-1R. *Org. Biomol. Chem. 14*, 2698–2705.

(35) Chang, C. L., Lien, E. J., and Tokes, Z. A. (1987) Synthesis, biological evaluation, and quantitative structure-activity relationship analysis of 2-hydroxy-1*H*-isoindolediones as new cytostatic agents. *J. Med. Chem. 30*, 509–514.

(36) Clegg, R. M. (1995) Fluorescence resonance energy transfer. *Curr. Opin. Biotechnol. 6*, 103–110.

(37a) Twumasi, D. Y., and Liener, I. E. (1977) Proteases from purulent sputum. Purification and properties of the elastase and chymotrypsin-like enzymes. *J. Biol. Chem. 252*, 1917–1926.

(b) Green, B. G., Weston, H.; Ashe, B. M.; Doherty, J.; Finke, P.; Hagmann, W.; Lark, M.; Mao, J.; Maycock, A.; Moore, V.; Mumford, R.; Shah, S.; and Knight, W. N. (1991) PMN elastases: a comparison of the specificity of human isozymes and the enzyme from other species toward substrates and inhibitors. *Arch. Biochem. Biophys. 286*, 284–292. (c) Watorek, W., van Halbeek, H., and Travis, J. (1993) The isoforms of human neutrophil elastase and cathepsin G differ in their carbohydrate side chain structures. *Biol. Chem. Seyler 374*, 385–393. (d) Dau, T., Sarker, R. S., Yildirim, A. O., Eickelberg, O., and Jenne, D. E. (2015) Autoprocessing of neutrophil elastase near its active site reduces the efficiency of natural and synthetic elastase inhibitors. *Nat. Commun. 6*, 6722.